Supplementary Information

Title

Formation mechanism of Ruddlesden-Popper faults in compressive-strained ABO_3 perovskite superlattices

Authors

Haoyuan Qi[1,2,*], Xiaodan Chen[1,3], Meng Wu[4], Eva Benckiser[4], Georg Christiani[4], Gennady Logvenov[4], Bernhard Keimer[4], Ute Kaiser[1,*]

Affiliations

[1]Central Facility of Materials Science Electron Microscopy, Universität Ulm, 89081 Ulm, Germany.

[2]Faculty of Chemistry and Food Chemistry & Center for Advancing Electronics Dresden (cfaed), Technische Universität Dresden, 01062 Dresden, Germany.

[3]Soft Condensed Matter, Debye Institute for Nanomaterials Science, Utrecht University, 3584 CC Utrecht, The Netherlands

[4]Max Planck Institute for Solid State Research and Center of Integrated Quantum Network, Heisenbergstraße 1, 70569 Stuttgart, Germany

*Corresponding authors: ute.kaiser@uni-ulm.de; haoyuan.qi@uni-ulm.de

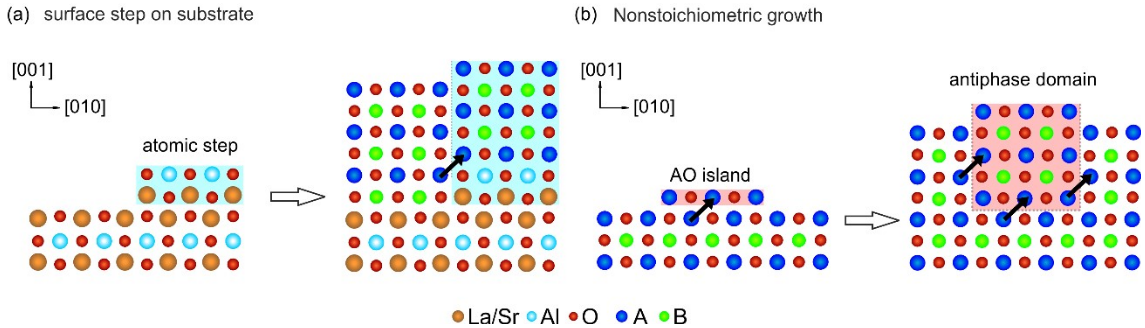

Fig. S1 (a) Formation of RP fault as a result of atomic steps on the surface of the $LaSrAlO_4$ substrate. Due to the rock-salt type structure of $LaSrAlO_4$, the atomic step is displaced with regard to the underlying layer by $a/2[111]$ (in pseudocubic axes). Subsequent deposition leads to an RP fault on the (010) plane. (b) Formation of RP fault due to nonstoichiometry. During the growth, the excessive A-site cations must be accommodated by the formation of an AO island on the fully coalesced AO layer. To minimize the electrostatic repulsion between the neighboring A-site cations, the AO island is displaced by $a/2[111]$ with respect to the underlying crystal, i.e., rock-salt type. The subsequent epitaxial growth results in an antiphase domain encompassed in RP faults on {100} planes.

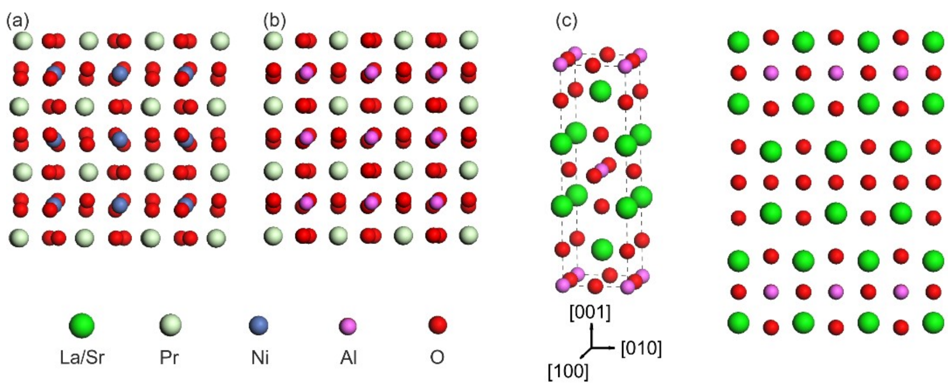

Fig. S2 (a) Atomic model of $PrNiO_3$ viewed in $[100]$ direction. The crystal can be described by a pseudocubic symmetry with the lattice parameter of $a_{PNO,pseudo}$= 3.82 Å (b) Atomic model of $PrAlO_3$ viewed in $[100]$ direction with $a_{PAO,pseudo}$ = 3.76 Å. (c) Atomic structure of the $LaSrAlO_4$ substrate. $LaSrAlO_4$ possesses tetragonal symmetry with $a = b = 3.75$ Å and $c = 12.65$Å.

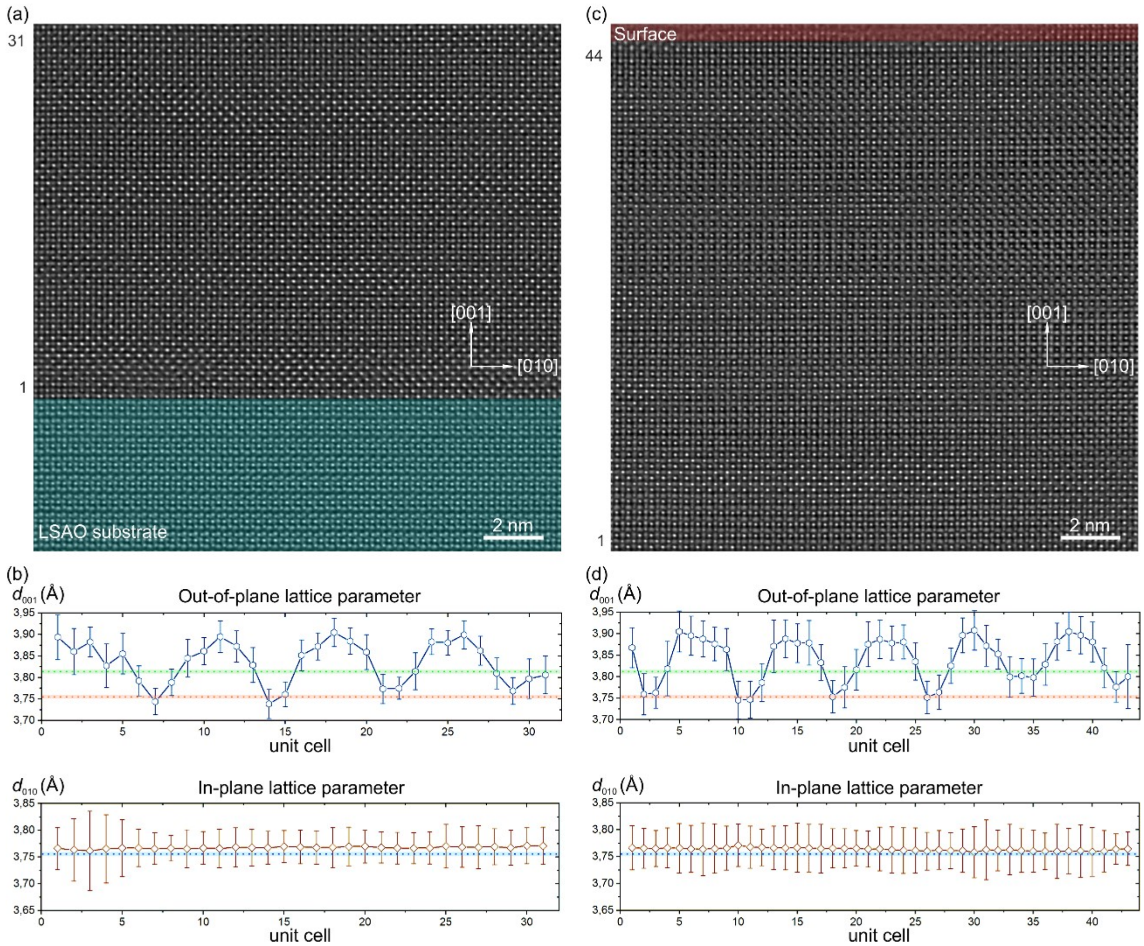

Fig. S3 (a) AC-HRTEM image acquired at the substrate-superlattice interface in [100] projection. Negative C_s imaging conditions have been applied with the spherical aberration coefficient C_s tuned to − 15 μm and an overfocus of c.a. 5 nm, resulting in bright-atom contrast. The number on the left denotes the numbering of unit cells along the growth direction [001]. (b) Measured out-of-plane lattice parameter d_{001} and in-plane lattice parameter d_{010} as a function of the number of unit cells along the growth direction. Each data point is averaged over 40 unit cells along the in-plane direction, and the error bar corresponds to the standard error. (c) AC-HRTEM image acquired at the superlattice surface. (b) Measured out-of-plane lattice parameter d_{001} and in-plane lattice parameter d_{010} as a function of the number of unit cells along the growth direction. d_{001} oscillates with a periodicity of 8 unit cells, agreeing well with the [4 u.c.//4 u.c.] $PrNiO_3/PrAlO_3$ bilayer structure.

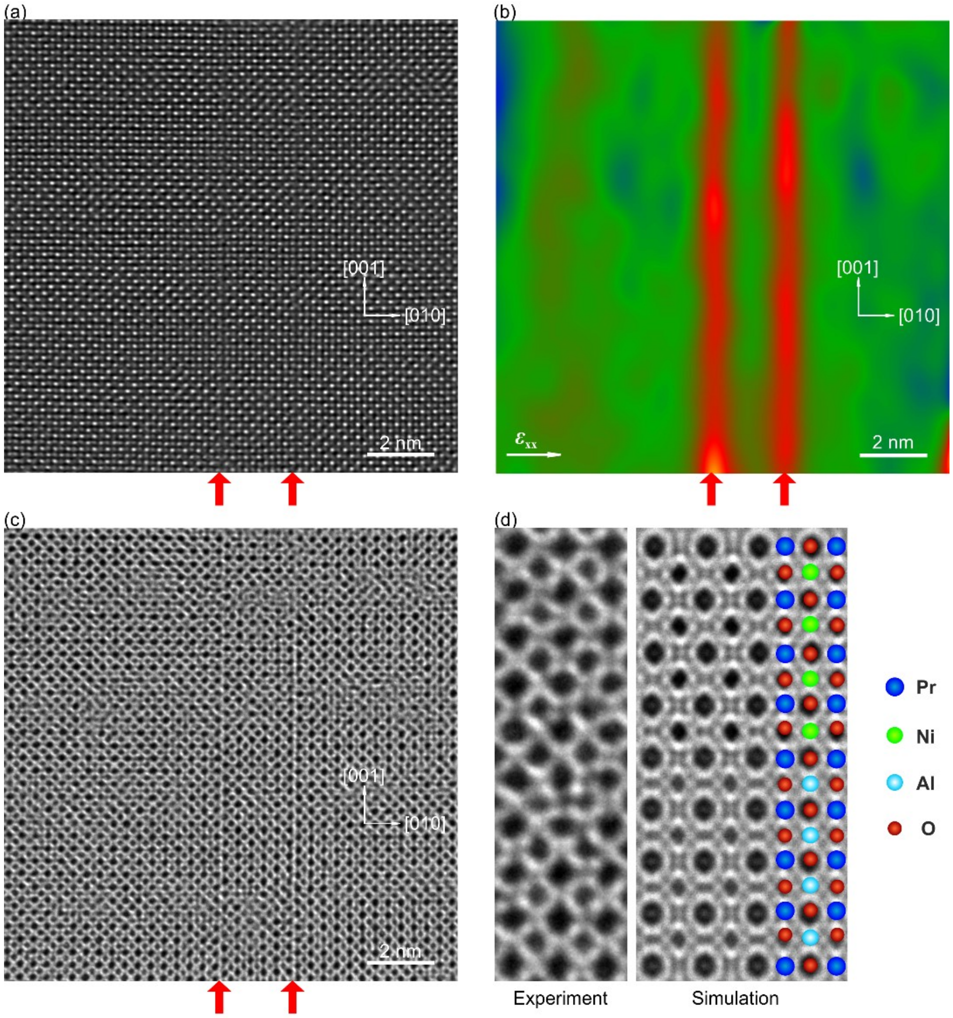

Fig. S4 (a) AC-HRTEM image acquired at the RP fault in [100] projection. Negative C_s imaging conditions has been applied with the spherical aberration coefficient C_s tuned to $-$ 15 µm and an overfocus of c.a. 5 nm, resulting in bright-atom contrast. The red arrows denote the RP fault plane. (b) In-plane strain map ε_{xx} showing a local expansion of the in-plane lattice parameter d_{020}. (c) AC-HRTEM image acquired at the same position as in (a). An underfocus of c.a. - 1 nm has been applied, resulting in dark-atom contrast. (d) Comparison between the experimental and simulated image, showing clear contrast distinction between Pr and Ni/Al cations.

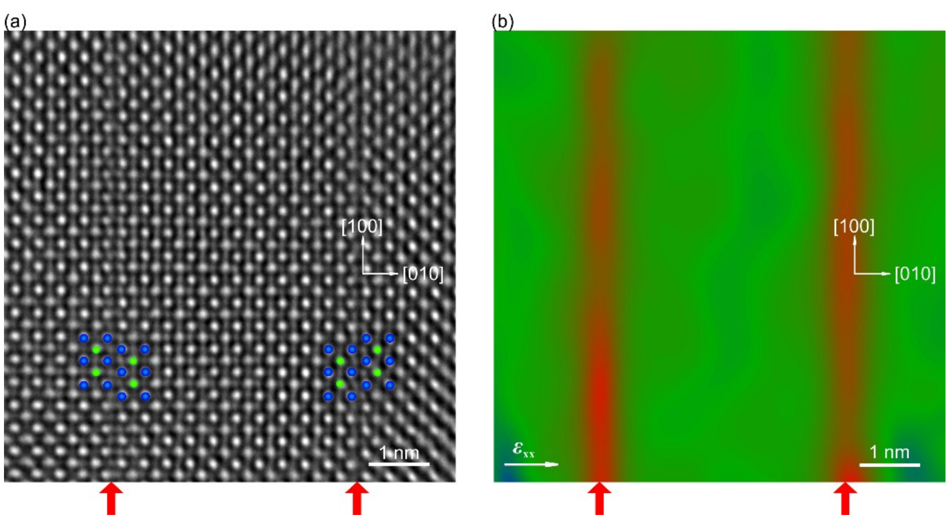

Fig. S5 (a) AC-HRTEM image acquired at the RP fault in [001] projection (i.e., plan view). The red arrows indicate the RP fault plane. (b) In-plane strain map ε_{xx} showing a local expansion of the in-plane lattice parameter d_{020}.

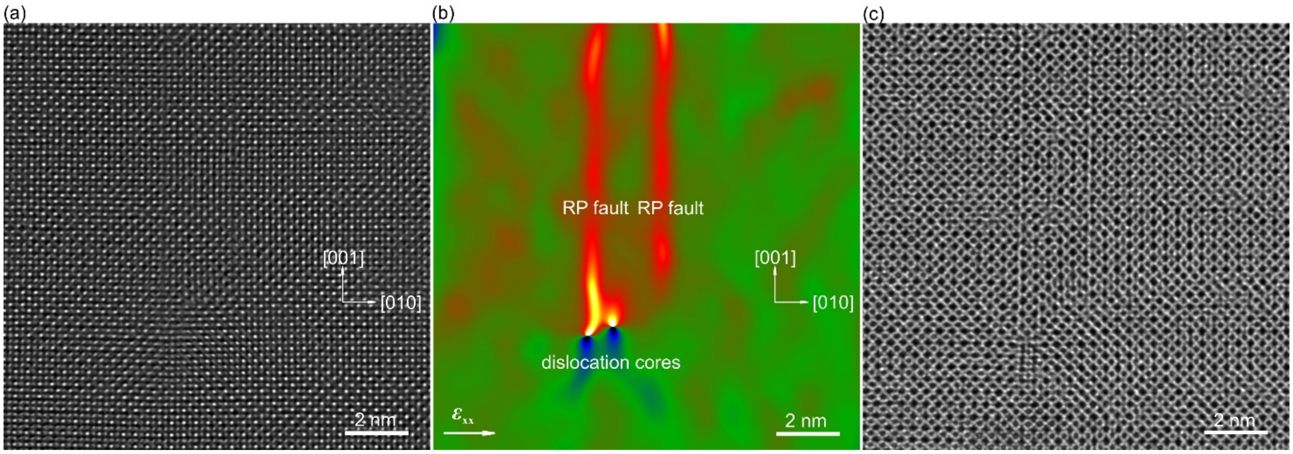

Fig. S6 (a) AC-HRTEM image acquired at the origin of the RP faults observed in Fig. 3 and S4. Negative C_s imaging conditions has been applied with the spherical aberration coefficient C_s tuned to − 15 µm and an overfocus of c.a. 5 nm, resulting in bright-atom contrast. (b) In-plane strain map ε_{xx} showing a local expansion of the in-plane lattice parameter d_{020} and two dislocation cores. (c) AC-HRTEM image acquired at the same position as in (a). An underfocus of c.a. - 1 nm has been applied, resulting in dark-atom contrast.

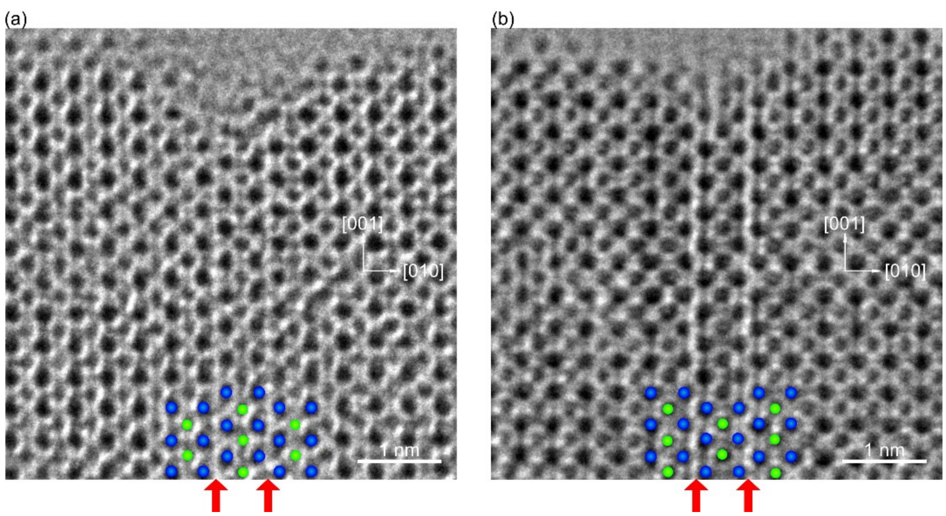

Fig. S7 AC-HRTEM images acquired with dark-atom contrast showing RP faults (indicated by the red arrows) separated by only 1 unit cell. No further broadening was observed till the superlattice surface.